Phase diagram and non-Abelian symmetry locking for fermionic mixtures with unequal interactions

Joao C. Pinto Barros
SISSA and INFN, Sezione di Trieste, Via Bonomea 265, I-34136 Trieste, Italy

Luca Lepori
Dipartimento di Scienze Fisiche e Chimiche, Università dell'Aquila, via Vetoio, I-67010 Coppito-L'Aquila, Italy;
INFN, Laboratori Nazionali del Gran Sasso, Via G. Acitelli, 22, I-67100 Assergi (AQ), Italy;
and Dipartimento di Fisica e Astronomia, Universita di Padova, Via Marzolo 8, I-35131 Padova, Italy

Andrea Trombettoni
CNR-IOM DEMOCRITOS Simulation Center, Via Bonomea 265, I-34136 Trieste, Italy
and SISSA and INFN, Sezione di Trieste, Via Bonomea 265, I-34136 Trieste, Italy
(Received 29 July 2016; published 5 July 2017)

The realization of experiments in ultracold multicomponent mixtures, also involving more atomic species, opened the way to the study of exotic quantum phases and unconventional superfluidity, as, for instance non-Abelian superfluid phases. In this paper we study the occurrence of non-Abelian symmetry-locked superfluid states in ultracold fermionic mixtures with four components, showing that such states can be studied in current day experiments with ^{171}Yb-^{173}Yb isotopes. We study the phase diagram in the presence of an attractive interaction between the species of two pairs of the mixture, and general (also repulsive) interactions between the species of each pair. This system can be physically realized, e.g., in mixtures of two different earth-alkaline species, both of them with two hyperfine levels selectively populated. We find an extended region of the diagram exhibiting a two-flavors superfluid symmetry-locking (TFSL) phase. The locking corresponds to the presence of a order parameter involving—in all the possible and distinct permitted ways—two fermions, one of them belonging to the first pair and the second to the other one. This TSFL phase is present also for not too large repulsive intrapair interactions and it is characterized by a global non-Abelian symmetry group obtained by locking together two independent invariance groups of the corresponding normal state. Explicit estimates are reported for the mixture of the fermionic isotopes ^{171}Yb-^{173}Yb, indicating that the TFSL phase can be achieved also without tuning the interactions between Yb atoms.

DOI: 10.1103/PhysRevA.96.013603

I. INTRODUCTION

Ultracold atoms provide an ideal playground for the simulation of strongly interacting quantum systems [1], mainly due to their high tunability and to the variety of the measurements that can be performed on such systems. Two ingredients greatly increase the versatility of ultracold atomic systems: optical lattices [2] and gauge potentials [3]. The wide class of phenomena that have been or may be studied using optical lattices include Mott-superfluid transitions [4], Josephson physics [5], and Hubbard physics in fermionic mixtures [6].

Regarding gauge potentials, the internal degrees of freedom coupled with them are in general hyperfine levels of certain atoms [7]. At the present time mostly static gauge potentials have been realized experimentally; however, in past years, proposals for dynamic gauge fields also appeared [8–12] and recently the first experimental realization has been performed [13].

In strongly correlated condensed-matter physics, gauge theories occur as effective models [14]. In this respect, the synthesis of Abelian and non-Abelian gauge potentials and fields, possibly on optical lattices [15–19], is expected to boost in the near future the investigation of a larger set of interesting systems, phenomena, and phases.

The realization of gauge potentials and fields points to the simulation of systems relevant for high-energy physics, namely strongly coupled field theories like quantum chromodynamics (QCD). The possibility of bringing, in an ultracold laboratory, paradigmatic models of high-energy physics has been discussed intensively in recent years. Notable proposals on this topics concern a variety of phenomena and models, including two-dimensional (2D) [20–27] and 3D [28–30] Weyl and Dirac fermions, symmetry-locked phases [31], and Schwinger pair production [32]. Theoretical proposals came along with experimental achievements, including the realization of Dirac fermions in honeycomb lattices [33], of the topological Haldane model [34], and of the Schwinger model [13]. Finally, ultracold fermions proved very useful to explore the unitary limit [35]: large interactions of the unitary limit could be used as a tool to construct toy models for quark confinement, chiral symmetry breaking, and string breaking.

Ultracold multicomponent mixtures, including quantum gases where more atomic species are simultaneously trapped, also opened in a natural way the possibility to study exotic phases and unconventional superfluidity [36]. In this paper we are interested in the realization of non-Abelian superfluid phases, focusing in particular on the so-called symmetry-locked phases. Such phases are realizable in suitable fermionic mixtures in which the components can be divided in two subsets, and they are induced by a order parameter connecting fermions belonging to the different subsets. The peculiar property of this parameter is that it involves all the possible pairing channels permitted by the symmetry of the system.

From a more general point of view, symmetry locking, a central concept for various areas of high-energy physics, occurs in the presence of a phase (typically superfluid), characterized by a particular nonvanishing vacuum expectation value, acting as an order parameter and inducing a suitable spontaneous symmetry-breaking pattern. Indeed, because of this expectation value, two independent symmetry groups of the normal phase are mixed in a residual symmetry subgroup.

In the system considered in the present paper, we study the dynamics of four fermionic components, generically divided in two subsets conventionally denoted as c and f. There a symmetry locking occurs in the presence of a nonvanishing order parameter between two atoms (one belonging to c and the other to f) such that this parameter involves all the possible pair configurations permitted by the symmetry of the normal phase.

Symmetry locking results in a number of peculiar properties, especially when the locked groups are non-Abelian, for instance, ordered structures as nets and crystals [37,38] or vortices and monopoles with semi-integer fluxes, confining non-Abelian modes [39–43]. A remarkable example of this phenomenon appears in the study of nuclear matter under extreme conditions, as in the core of ultradense neutron stars [44]. There the locking interests the $\mathrm{SU}(3)_c$ (local) color and the $\mathrm{SU}(3)_f$ (global) flavor groups. Similarly the chiral symmetry-breaking transition involves a locking of global left $\mathrm{SU}(3)_L$ and right $\mathrm{SU}(3)_R$ flavor symmetries [37,38].

A step forward towards the study of symmetry-locked states was provided in [31], based on multicomponent fermionic mixtures: there a proposal for the synthesis of a superfluid phase locking two non-Abelian global symmetries has been presented. This state has been denoted as a two-flavor symmetry-locked (TFSL) state. In the analysis presented in [31] it was considered a four component mixture with attractive Hubbard interactions between the species in two subsets (denoted by c and f) of the mixture (the interaction coefficient being denoted by $U_{cf} > 0$) and attractive interactions between the species of each subset (respectively $U_c > 0$ and $U_f > 0$). With $U_c = U_f \equiv U$ and $U_{cf} > U$ the mixture hosts very peculiar phenomena significant for high-energy physics, such as TFSL states, fractional vortices, and non-Abelian modes confined on them [31]. Beyond its intrinsic interest, this scheme represents a first step towards the simulation of phases involving the breaking of local (gauge) symmetries, as in the QCD framework.

Multicomponent fermionic mixtures appear to be a natural playground to simulate symmetry locking. One notable example is given by multicomponent Yb gases, that can be synthesized and controlled at the present time [45]. Yb atoms, as all the earth-alkaline atoms, have the peculiar property that their interactions do not depend on the hyperfine quantum number labeling the states of a certain multiplet. This fact allows one to realize interacting systems, bosonic and fermionic, with non-Abelian $\mathrm{U}(N)$ or $\mathrm{SU}(N)$ symmetries [46] whose generators act on the hyperfine space. In particular, one can think to realize the desired four component mixture using fermionic ^{171}Yb and ^{173}Yb atoms [31]. Each species is selectively populated in two different hyperfine levels and loaded on a cubic optical lattice. Although the scattering length $a_{171-173}$ between ^{171}Yb and ^{173}Yb atoms is negative and rather large ($a_{171-173} = -578\,a_0$, with a_0 the Bohr radius) resulting in an attractive interaction $U_{cf} > 0$, the scattering length $a_{171-171}$ between ^{171}Yb atoms is small and negative ($a_{171-171} = -3\,a_0$) giving $U_c \approx 0$, and the scattering length $a_{173-173}$ between ^{173}Yb atoms is *positive* and much larger than $a_{171-171}$ ($a_{173-173} = +200\,a_0$) resulting in $U_f < 0$, i.e., a repulsion [47].

In the case discussed above, an attractive interaction between the ^{171}Yb and ^{173}Yb atoms favors the symmetry-locked phase, while a too strong attraction or repulsion between the populated hyperfine levels of ^{171}Yb or of ^{173}Yb may spoil it. Therefore, a natural question is to what extent the TFSL phase can remain stable. This question fits into the more general problem of determining the phase diagram and the actual extension of the TFSL phase as the interactions between the atoms of the considered four-component mixture are varied.

In order to settle these questions, in the present paper we explore the phase diagram of a four-component mixture with attractive interpair interaction. We consider general (also repulsive) interactions between the species of the pairs, clarifying the ranges for the experimental parameters where a TFSL phase can occur. By our study we conclude that a TFSL phase could be synthesized in a close future, using already reachable values of the experimental parameters like the lattice widths. Notably this task can be achieved just assuming the natural interactions of ^{171}Yb and ^{173}Yb atoms, without any external tuning. Indeed, for instance, the critical temperature required to enter in the superfluid TFSL phase turns out of the same order of the ones presently reached. This result is particularly relevant in the light of the known difficulty to tune interactions between earth-alkaline atoms, as the Yb, without destructing their $\mathrm{U}(N)$ invariance and avoiding important losses of atoms or heating in the experimental setups.

II. MODEL

We consider a four-species fermionic mixture involving atoms in two different pairs of states (possibly pairs of hyperfine levels). For convenience we label the four degrees of freedom as $\sigma \in \{r,g,u,d\}$ and distinguish between the species $\{r,g\}$ in the first pair c and the species $\{u,d\}$ in the second pair f.

Even if the mechanism we are going to describe is independent on the space where the atoms are embedded, in the following the mixture will be considered to be loaded in a cubic optical lattice. A discussion of possible advantages of this choice will be presented in Sec. V. The system is described by a Hubbard-like Hamiltonian $H = H_{\mathrm{kin}} + H_{\mathrm{int}}$,

$$H_{\mathrm{kin}} = -t \sum_{\langle i,j\rangle,\sigma} c^{\dagger}_{i\sigma} c_{j\sigma},$$
$$H_{\mathrm{int}} = -\sum_{i,\sigma\sigma'} U_{\sigma\sigma'} n_{i\sigma} n_{i\sigma'} \qquad (1)$$

(with $t > 0$). The matrix $U_{\sigma\sigma'}$ is symmetric with vanishing diagonal elements (because of the Fermi statistics).

We are interested in particular in a situation where the interactions between the multiplets c and f do not depend on the specific levels chosen in each pair. As mentioned in the Introduction, an experimental realization of this condition

is performed by using earth-alkaline atoms. For instance, a specific proposal relies on the use of the two hyperfine levels of ^{171}Yb and of two suitably chosen levels in the six-multiplet of ^{173}Yb. More details on this mixture will be given in Sec. V; see as well [48].

The system in Eq. (1) is therefore characterized by three interaction parameters labeled as $U_{rg} \equiv U_c$, $U_{ud} \equiv U_f$, and $U_{ru} = U_{rd} = U_{gu} = U_{gd} \equiv U_{cf}$. In the following we will refer to the interactions associated with U_c and U_f as "intrapair" interactions and to the ones associated with U_{cf} as "interpair" interactions. Notice the convention used in Eq. (1), where the interaction term is proportional to $-U_{\sigma\sigma'}$, so that positive values for $U_{\sigma\sigma'}$ correspond to attractions. In particular, to have a TSFL phase we need U_{cf} positive and large enough.

Once the hoppings and the occupation numbers of the species are set equal in each multiplet, the system in the normal (Fermi liquid) state has a group symmetry $\mathcal{G} = \mathrm{U}(2)_c \times \mathrm{U}(2)_f$ corresponding to *independent* rotations on the c and f degrees of freedom, respectively. More in detail, these transformations act as

$$\begin{pmatrix} c_1' \\ c_2' \end{pmatrix} = \mathcal{U}_c \begin{pmatrix} c_1 \\ c_2 \end{pmatrix}, \tag{2}$$

where $\mathcal{U}_c = e^{i\,\vec{\theta}_c\cdot\vec{\sigma}}$, $\vec{\sigma}$ are the Pauli matrices, and $\vec{\theta}_c$ a vector having as components some free parameters. The same action and form hold for $\mathcal{U}_f$. The invariance under $\mathcal{U}_{c,f}$ means that

$$\mathcal{U}_c\, H\, \mathcal{U}_c^{-1} = H \tag{3}$$

and

$$\mathcal{U}_f\, H\, \mathcal{U}_f^{-1} = H. \tag{4}$$

On the contrary, as shown in Ref. [31], when superfluidity is induced, $\mathcal{G}$ may undergo in general a spontaneous symmetry breaking into a smaller subgroup H. In particular, when superfluidity occurs between the c and the f atoms, the following spontaneous symmetry breaking (SSB) [49] pattern takes place:

$$\mathrm{U}(2)_c \times \mathrm{U}(2)_f \to \mathrm{U}(2)_{c+f}. \tag{5}$$

This means that the superfluid phase displays a (continuous) set of unitary equivalent but physically inequivalent degenerate ground states, characterized by a matrix gap parameter Δ_{cf} It transforms under a generic element $(\mathcal{U}_c,\mathcal{U}_f)$ of G as $\mathcal{U}_c\,\Delta_{cf}\,\mathcal{U}_f^{-1}$. However, this matrix has a residual invariance, under the non-Abelian subgroup $\mathcal{H} = \mathrm{U}(2)_{c+f} \in \mathrm{U}(2)_c \times \mathrm{U}(2)_f$ acting as follows:

$$\mathcal{U}_c\,\Delta_{cf}\,\mathcal{U}_c^{-1} = \mathcal{U}_f^{-1}\,\Delta_{cf}\,\mathcal{U}_f = \Delta_{cf}. \tag{6}$$

Notably $\mathcal{H} = \mathrm{U}(2)_{c+f}$ involves at the same time c and f transformations, originally independent. For this reason the described pattern of SSB is called symmetry locking (see, e.g., Ref. [44]).

The mentioned relevance and generality of the symmetry-locking phenomenon, as well as the intrinsic interest for non-Abelian superfluid phases, motivate an effort to realize the model in Eq. (1) in current ultracold atoms experiments.

III. MEAN-FIELD ENERGY AND CONSISTENCY EQUATIONS

In the present section we consider the possible emergence of superfluid states, with various (numbers of) pairings in the system described by Eq. (1), investigating more in general the superfluid BCS phases that can arise in it. We start the analysis by using a mean-field approximation, and we present strong-coupling results in Sec. IV.

In the mean-field approximation the energy $\mathcal{F}$ at zero temperature can be written as

$$\mathcal{F} = \frac{1}{2}\sum_{\vec{k}} \hat{\psi}_{\vec{k}}^{\dagger}\, F_{\vec{k}}\, \hat{\psi}_{\vec{k}} + F_c, \tag{7}$$

where $\hat{\psi}_{\vec{k}}^{\dagger} = (c_{kr}\ldots c_{kd}, -c_{-kr}^{\dagger}\ldots - c_{-kd}^{\dagger})$, and $F_{\vec{k}}$ is the 8×8 matrix:

$$F_{\vec{k}} = \begin{pmatrix} \xi_{\vec{k},\{\sigma\}} & 2\Delta_{\sigma\sigma'} \\ 2\Delta_{\sigma\sigma'}^{*} & -\xi_{\vec{k},\{\sigma\}} \end{pmatrix}. \tag{8}$$

The indices σ,σ' on $\Delta_{\sigma\sigma'}$ run through the labels $\sigma \in \{r,g,u,d\}$, $\Delta_{\sigma\sigma'}$ being therefore a 4×4 matrix. The factor 2 in front of $\Delta_{\sigma\sigma'}$ is due to the double sum in Eq. (1). Moreover,

$$\xi_{\vec{k}\sigma} = \mathrm{diag}(\varepsilon_{\vec{k}} - \tilde{\mu}_\sigma),$$

where

$$\varepsilon_{\vec{k}} = -2t\sum_{l=1}^{3} \cos k_l$$

and

$$\tilde{\mu}_\sigma = \mu_\sigma + \nu_\sigma U_\sigma + 2\nu_{\bar{\sigma}} U_{cf} \tag{9}$$

are the chemical potentials shifted by the Hartree terms. In Eq. (9) ν_σ denote the fillings and $\bar{\sigma}$ denotes the "opposite" degree of freedom, so if σ is a c index then $\bar{\sigma}$ is an f and vice versa. As we are interested in the case $\nu_r = \nu_g = \nu_c/2$ and $\nu_u = \nu_d = \nu_f/2$, there is no ambiguity on the definition of $\bar{\sigma}$. Notice that here we assume, unless otherwise specified, the balance between the two c and the two f species separately (this is the origin of the 2 factor in front of $\nu_{\bar{\sigma}}\,U_{cf}$ in the expression above for $\tilde{\mu}_\sigma$).

The constant F_c in Eq. (7) is defined as follows:

$$F_c = \frac{1}{2}\sum_{\vec{k},\sigma}\xi_{\vec{k}\sigma} + V\sum_{\sigma\neq\sigma'} U_{\sigma\sigma'}^{-1}|\Delta_{\sigma\sigma'}|^2, \tag{10}$$

with V being the number of lattice sites, $\langle c_{k\sigma}^{\dagger} c_{k\sigma'}\rangle = \delta_{\sigma\sigma'} n_\sigma$ and $\Delta_{\sigma\sigma'} \equiv -V^{-1}\,U_{\sigma\sigma'}\sum_{\vec{k}}\langle c_{k\sigma}\,c_{-k\sigma'}\rangle$, assumed real. The matrix Δ_{cf}, introduced in Eq. (6), is as a 2×2 matrix with entries $[\Delta_{\mathbf{cf}}]_{\sigma_c\sigma_f} = -V^{-1}\,U_{cf}\,\sum_{\vec{k}}\langle c_{k\sigma_c} c_{-k\sigma_f}\rangle$, where σ_c and σ_f belong respectively to the sets $\{r,g\}$ and $\{u,d\}$. Moreover, $\mu_r = \mu_g \equiv \mu_c$ and $\mu_u = \mu_d \equiv \mu_f$.

The problem in describing superfluid phases of the Hamiltonian in Eq. (1) is then reduced, at the mean-field level, to the diagonalization of $F_{\vec{k}}$ and to the subsequent determination of $\Delta_{\sigma\sigma'}$ and $\tilde{\mu}_\sigma$ by the solution of self-consistent equations. If more solutions are found, one has to find the one having smaller energy.

The energy of the system can be found diagonalizing the matrix $F_{\vec{k}}$ and obtaining its eigenvalues $\lambda_{\vec{k},\alpha}$, with

$\alpha = 1, \ldots, 8$. These eigenvalues can be divided in two sets with opposite sign and equal magnitude. Putting the resulting diagonal form of $\mathcal{F}$ in normal order all the energies are defined positive; moreover, in this way the constant term F_c gets shifted: $F_c \to F_c - \sum_{\vec{k},\alpha} \frac{\lambda^{(+)}_{\vec{k},\alpha}}{2}$, where $\lambda^{(+)}_{\vec{k},\alpha}$ denote the four positive eigenvalues of $F_{\vec{k}}$.

The ground-state energy is found to be

$$F_c = \frac{1}{2}\sum_{\vec{k}}\left(\sum_{\sigma}\xi_{\vec{k}\sigma} - \sum_{\alpha}\lambda^{(+)}_{\vec{k}\alpha}\right) + V\sum_{\sigma\sigma'}U^{-1}_{\sigma\sigma'}|\Delta_{\sigma\sigma'}|^2. \tag{11}$$

The self-consistent equations for $\Delta_{\sigma,\sigma'}$ and the shifted chemical potentials $\tilde{\mu}_\sigma$ can now be obtained from the conditions

$$\frac{\partial F_c}{\partial \Delta_{\sigma,\sigma'}} = 0,$$
$$\frac{\partial (F_c + \tilde{\mu}_\sigma n_\sigma)}{\partial \tilde{\mu}_\sigma} = 0. \tag{12}$$

Several solutions of Eqs. (12) are possible in general. For this reason, in order to fix the correct phase for every point $(\frac{U_c}{t}, \frac{U_f}{t}, \frac{U_{cf}}{t})$ of the diagram, one has to find the lowest-energy solution.

We distinguish the various solutions as follows:

(i) Normal: no superfluid pairing exist between any degrees of freedom. That means $\Delta_{\alpha\beta} = 0$ for any pair (α,β).

(ii) Non-TFSL (NTFSL): intrapairing occurs but interpairing does not: $|\Delta_{c_1c_2}|^2 + |\Delta_{f_1f_2}|^2 \neq 0$ and $\Delta_{cf} = 0$. In this case the two nontrivial Bogoliubov energies entering Eq. (11) read $\lambda^{(+,c)}_{\vec{k}\alpha} = \sqrt{\xi^2_{\vec{k}} + |\Delta_{c_1c_2}|^2}$ and $\lambda^{(+,f)}_{\vec{k}\alpha} = \sqrt{\xi^2_{\vec{k}} + |\Delta_{f_1f_2}|^2}$.

(iii) TFSL: interpairing occurs but intrapairing does not: $|\Delta_{c_1c_2}|^2 + |\Delta_{f_1f_2}|^2 = 0$ and $\Delta_{cf} \neq 0$. In this case the two nontrivial Bogoliubov energies entering Eq. (11) read $\lambda^{(+)}_{\vec{k}\alpha} = \sqrt{\xi^2_{\vec{k}} + |\Delta_{cf}|^2}$, with $\Delta_{cf} = \frac{1}{2}\mathrm{Tr}\Delta_{cf}$ being Δ_{cf}.

Solving numerically Eqs. (12), it turns out that whenever in the presence of an attractive interpair interaction ($U_{cf} > 0$), a solution with nonzero pairing $\Delta_{\sigma\sigma'}$ and energy lower than the one for the normal state always exists. Therefore, the normal state solution, even though always present, is never favored. This result then assures the existence of a superfluid state, also in the presence of intrapair repulsion. Of course, this is a mean-field result for the considered model, expected not to be correct for large intrapair repulsions: a strong-coupling analysis of such a case is presented in Sec. IV.

The obtained superfluid BCS solutions are always of the TFSL or NTFSL types; in other words, no solution with both $|\Delta_{c_1c_2}|^2 + |\Delta_{f_1f_2}|^2 \neq 0$ and $\Delta_{cf} \neq 0$ occurs. We observe that, setting $n_c = n_f$ for all the three mentioned types of solutions, the shifted chemical potentials $\tilde{\mu}_c$ and $\tilde{\mu}_f$ turn out equal, in spite of the intrapair interactions U_c and U_f, different in general. In particular, they depend only on n_c and n_f themselves. This means that, at least at the mean-field level, these interactions do *not* determine any effective unbalance between the c and f species. This fact is expected to remain at least approximatively true in the presence of a trapping potential, since this potential acts, in local density approximation, as a space-dependent correction to the chemical potentials $\mu_{c,f}$ at the center of the trap [50], not to the shifted potentials $\tilde{\mu}_{c,f}$. This appears particularly relevant since it is known (see [50] and references therein) that generally an unbalance in the normal state can spoil the possible emergence of superfluid states, or at least modify the critical interaction strength and the critical temperature.

For the case $n_c = n_f \equiv n$, it is true that $\xi_{\vec{k},\sigma} \equiv \xi_{\vec{k}}$ and it is possible to recast the self-consistency Eqs. (12) in a BCS-like form:

$$1 = \frac{U_{c,f}}{V}\sum_{\vec{k}}\frac{1}{\sqrt{\xi^2_{\vec{k}} + 4|\Delta_{c,f}|^2}}, \quad \Delta_{cf} = 0, \quad \text{NTFSL} \tag{13}$$

or

$$1 = \frac{U_{cf}}{V}\sum_{\vec{k}}\frac{1}{\sqrt{\xi^2_{\vec{k}} + 4|\Delta_{cf}|^2}}, \quad \Delta_{c,f} = 0, \quad \text{TFSL} \tag{14}$$

(recall that $\Delta_{cf} = \mathrm{Tr}\,\Delta_{\mathrm{cf}}/2$) and

$$n_\theta = \frac{1}{V}\sum_{\vec{k}}\left(1 - \frac{\xi_{\vec{k}}}{\sqrt{\xi^2_{\vec{k}} + 4|\Delta_\theta|^2}}\right). \tag{15}$$

For the sake of brevity, in the last equation Δ_θ is meant to include both Δ_{cf} and Δ_c, Δ_f, corresponding to both the cases TFSL and NTFSL. Notice that Eqs. (13)–(15) reproduce exactly the standard BCS self-consistency equations, as one should expect: indeed the different numerical factors in Eqs. (13)–(15) are due to the different definitions for U_c, U_f, U_{cf} and the corresponding gap parameters used here.

IV. PHASE DIAGRAM

In this section we use Eqs. (11) and (12) to investigate the phase diagram of the Hamiltonian (1) as a function of the external parameters t, U_c U_f, and U_{cf}. In particular, we numerically solve Eqs. (12) for a cubic lattice having 20^3 sites (checking that the phase diagram is not affected by finite-size effects), and we compare the energies of the obtained solutions to determine the mean-field phase diagram. Later in the text we discuss limitations of the mean-field findings and an alternative approach to study the case of large intrapair repulsive interaction.

A. Attractive U_c, U_f

The results presented in Fig. 1 refer to the half-filling case ($n_\sigma = \frac{1}{2}$, corresponding to $n_c = n_f \equiv n = 1$) and different values of the ratio U_{cf}/t and U_c/t, U_f/t. In this case we always find $\tilde{\mu}_\sigma = 0$, as required by particle-hole symmetry (see, e.g., Ref. [51]).

For each fixed value of $U_{cf}/t > 0$ (attractive regime) a colored curve is drawn, separating the TFSL phase inside of it from the NTFSL phase outside. We see that, as we increase the value of U_{cf}/t, higher values of attractive intrapair couplings U_c/t, U_f/t are required to break the TFSL phase in favor of the NTFSL one. At variance the normal state is never favored over both the superfluid states, even when one of or both the intrapair interactions are repulsive and not small in comparison with the attractive ones. In this case the mean-field approach

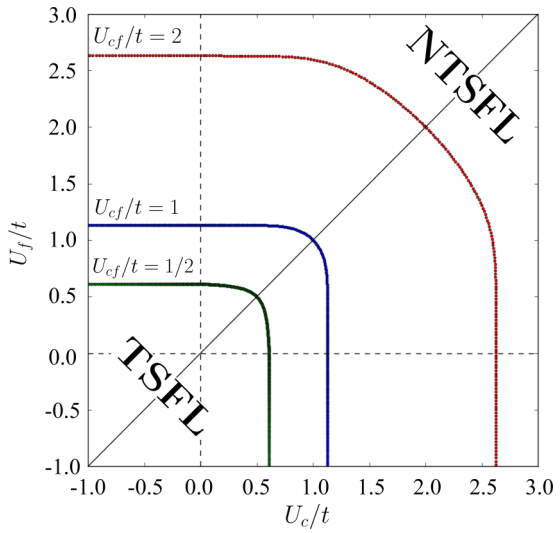

FIG. 1. Phase diagram at half filling for $U_{cf}/t = \{1/2, 1, 2\}$. Inside the curves (at smaller values of U_σ) the TFSL phase occurs, while outside one has the NTFSL phase. As U_{cf}/t increases, the zone of the TFSL phase becomes larger.

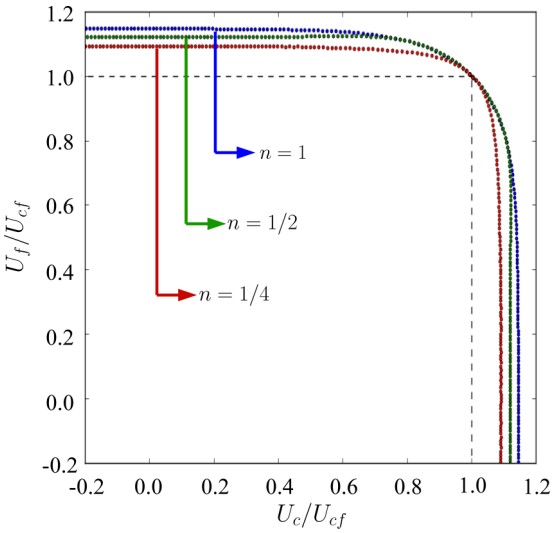

FIG. 3. Phase diagrams for $U_{cf}/t = 1$ and at different fillings: $n = 1$ (blue), $n = 1/2$ (green), and $n = 1/4$ (red). They appear qualitatively very similar indicating that the filling does not play a fundamental role.

is expected not to be reliable and, as we will see in the next subsection, antiferromagnetic states can be instead favored.

In Fig. 2 the curves of Fig. 1 are rescaled by their values of U_{cf}/t. With such a rescaling, all the curves meet in the point $U_c = U_f = U_{cf}$. In this point all the different Hamiltonians have a U(4) symmetry and the two phases TFSL and NTFSL can be mapped onto each other, signaling a transition point between the two phases, in agreement with [31].

The black point in Fig. 2 represents the case of the mixture composed by ^{171}Yb and ^{173}Yb, where natural interactions between these isotopes are assumed. This mixture, mentioned in Sec. I, will be discussed in detail in Sec. V. Here we notice only that the point lies well inside the TFSL zone.

The phase diagram shown in Fig. 2 is not a consequence of the hypothesis of half-filling or of balanced mixture. Indeed in Fig. 3 we plot the same phase diagram for different fillings (but still equal for the four species), finding qualitative agreements with small quantitative differences. Similarly, in Fig. 4 the case where the pairs c and f have fillings differing by 10% is reported. Again we see that the imbalance in the populations does not produce significative differences on the results. We stress that, although an imbalance in the number of particles is generally known able to spoil the appearance of superfluid states [50], in the present case the reliability of our results

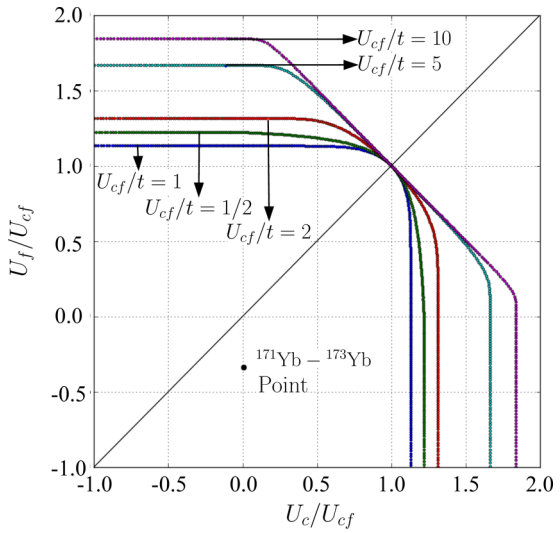

FIG. 2. Phase diagram in units of U_{cf} at half filling. The point $U_c = U_f = U_{cf}$ is a transition point between the phases TFSL and NTFSL, irrespective of the value for t. The point representing the natural interactions of the mixture ^{171}Yb-^{173}Yb is also depicted [48]. The corresponding estimates for this point are performed in Sec. V.

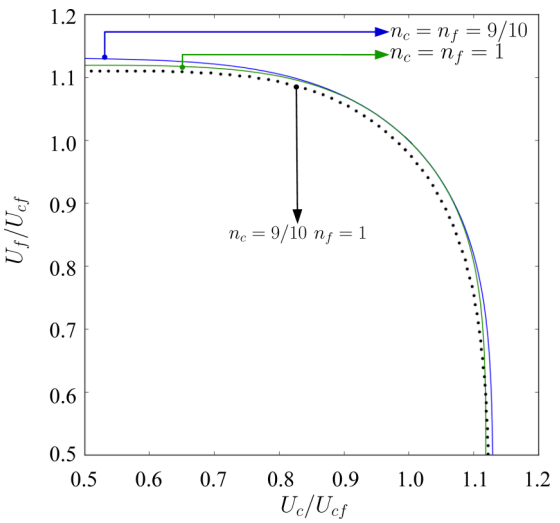

FIG. 4. Phase diagram in the presence of a small unbalance between the populations $n_f - n_c = 0.1$ and $U_{cf} = t$. The result is qualitatively very similar to the balanced cases (see also Figs. 2 and 3).

is guaranteed by the absence of other nontrivial solutions for the Eqs. (12) (see, for comparison, e.g., Ref. [52]) and by the direct comparison between the energies of the normal states and the one of the BCS-like superfluid solutions.

B. Repulsive U_c, U_f

When U_c, U_f assume negative values and repulsive intrapair interactions appear in the Hamiltonian of Eq. (1), the formation of intrapair pairs start to become suppressed. However, the normal state is never favored in the mean-field approximation as shown in Figs. 1–4.

If it is reasonable that for small intrapair repulsions the TFSL is favored, for large enough values of U_c/t, U_f/t and U_c/U_{cf}, U_f/U_{cf} this superfluid phase is expected to eventually disappear. The latter regime is qualitatively described in the strong-coupling limit U_c/t, U_f/t by spin Hamiltonians, similar to the Heisenberg model for a two species repulsive mixtures at half filling (see, e.g., Ref. [51]).

In the strong-coupling limit two cases are explicitly considered here: (a) $|U_c|/t, |U_f|/t \gg 1$; (b) $|U_c|/t \ll 1$ and $|U_f|/t \gg 1$. Notice that in both cases the further condition $|U_c/U_{cf}|, |U_f/U_{cf}| \gg 1$ is implicitly assumed.

In the first case the strong-coupling Hamiltonian reads (details of the derivation are in Appendix A)

$$\hat{H}^{cf}_{\text{eff}} = \frac{t^2}{4}\sum_{\langle i,j\rangle}\left(\frac{1}{|U_c|}\vec{C}_i\cdot\vec{C}_j + \frac{1}{|U_f|}\vec{F}_i\cdot\vec{F}_j\right) - E^{cf}_{GS}, \quad (16)$$

where $\vec{C}$ and $\vec{F}$ are effective spin variables defined by $\vec{S}_i = \sum_{\sigma\sigma'} c^\dagger_{i\sigma}\vec{\tau}_{\sigma\sigma'}c_{i\sigma'}$ ($\vec{\tau}$ denoting the Pauli matrices), the indices σ and σ' running through the labels c or f. E^{cf}_{GS} is the ground-state energy given by

$$E^{cf}_{GS} = -NU_{cf} - \frac{zNt^2}{4}\left(\frac{1}{|U_c|}+\frac{1}{|U_f|}\right), \quad (17)$$

where $N = 2V$ is the total number of atoms, corresponding therefore to half filling for each species of the four-component mixture. The Hamiltonian in Eq. (16) corresponds to two decoupled Heisenberg models.

The case (b) is of interest for the Yb discussed in the next section, in the perspective of a possible experimental realization for the TFSL mechanism. Here the ground-state energy is found in the limit $U_c/t \to 0$ (see details in Appendix B):

$$E^{c}_{GS} = 2E^{NS}_{GS} + \Delta E = 2E^{NS}_{GS} - N\left(\frac{U_c}{4} + \frac{z\,t^2}{4|U_f|}\right), \quad (18)$$

where E^{NS}_{GS} is the energy of a single c component in the normal state. Indeed the energy in Eq. (18) is proper of a system of free fermions c on an antiferromagnetic background describing the dynamics of the f fermions and described by a spin Hamiltonian similar to the one in Eq. (16).

The regions of the phase diagram where both the TFSL and NTFSL superfluid phases occur can be bounded comparing their ground-state energies with the energies of the antiferromagnetic phases in Eqs. (17) and (18).

Postponing the details for the case (b) to Sec. V, we present the results of this calculation for the case (a) in Fig. 5. There the oblique lines represent a set of points where, according to the energy criterium mentioned above, the insulator states become favorable over the superfluid phases. Notice that increasing the ratio U_{cf}/t results in an increase of the area of the TFSL phase, compared with the insulator one.

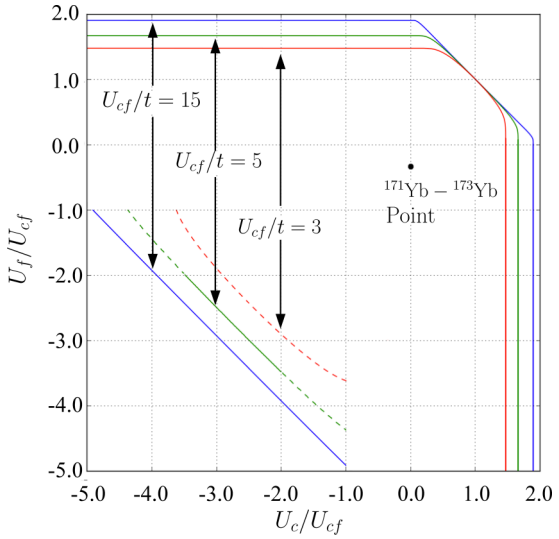

FIG. 5. Phase diagram, containing the natural point for the ytterbium mixture, for the cases $U_{cf} = 3t$ (red), $U_{cf} = 5t$ (green), and $U_{cf} = 15t$ (blue). The oblique lines bounding the superfluid phases are obtained by the strong-coupling approach leading to Eqs. (17) and (18). Dashed lines are used when the conditions $|U_c/t|, |U_f/t| \gg 1$ does not hold.

The calculations leading to Eqs. (17) and (18) are perturbative in t/U_σ; therefore, the comparison between the energies in the same equations and the ones for the superfluid states is reliable only $t/U_\sigma \ll 1$. For this reason a dashed line, instead of a solid one, is drawn in Fig. 5 where the condition $|t/U_\sigma| > 10^{-1}$ (a threshold conventionally chosen) starts to hold, so that the strong-coupling approach is no longer expected to be fully reliable. From the figure we see that for $U_{cf}/t = 3$ the transition line can never be located perturbatively, while for $U_{cf}/t = 15$ the converse is true. As an intermediate example $U_{cf}/t = 5$ exhibits both a zone where perturbation theory can be assumed valid and other ones where it cannot.

V. EXPERIMENTAL FEASIBILITY AND LIMITS

As mentioned in the previous sections, a possible experimental realization of the system investigated in the preceding section is provided by a mixture of ^{171}Yb and ^{173}Yb. The first isotope has a $1/2$ hyperfine multiplet, while the second one has $5/2$ hyperfine degeneracy. For the latter atomic species only two levels could be selectively populated. The mixture obtained in this way exhibits natural interactions characterized as follows: using conventionally the label c for the hyperfine levels of ^{171}Yb and the label f for the ones of ^{173}Yb, the scattering lengths are $a_c = -3a_0$, $a_f = 200a_0$, and $a_{cf} = -578a_0$, where a_0 is the Bohr radius (see, e.g., Refs. [47,48]). As in all the earth-alkaline atoms, the tunability of these interactions is very difficult using the magnetic Feshbach resonance, because of the negligible magnetic moment of such

atoms. Moreover, in the recent literature this problem revealed challenging also using alternative techniques, due to important atomic losses and without spoiling their characteristic U(N) invariance (N denoting here the number of hyperfine levels of the considered atomic species). For details on this subject see [53] and references therein. This problem can prevent the realization of certain phases and the exploration of the full phase diagram. For our purposes the question is then if, without tuning the interaction, the TFSL superfluid phase is realized or not.

For the considered earth-alkaline mixture loaded on a cubic lattice, the hopping parameters, in principle different, are given by

$$t_\alpha = -\int d^3\vec{r}\left(\frac{\hbar^2}{2m_\alpha}\nabla\phi_{\alpha\vec{r}'}(\vec{r})\cdot\nabla\phi_{\alpha\vec{r}''}(\vec{r}) + \phi_{\alpha\vec{r}'}(\vec{r})V_{\rm ext}(\vec{r})\phi_{\alpha\vec{r}''}(\vec{r})\right). \tag{19}$$

The expressions for the interaction parameters U_c, U_f, U_{cf} in the form of $U_{\alpha\beta}$ for $\alpha \neq \beta \in \{r,g,u,d\}$ are [notice the minus sign in Eq. (1)]

$$U_{\alpha\beta} = -\frac{\pi\hbar^2 a_{\alpha\beta}}{m_{\alpha\beta}}\int d^3\vec{r}\,|\phi_{\alpha\vec{r}'}(\vec{r})|^2|\phi_{\beta\vec{r}'}(\vec{r})|^2. \tag{20}$$

In Eqs. (19) and (20), $\phi_{\{\alpha,\beta\}\vec{r}'}(\vec{r})$ are the Wannier functions describing the localization on a given lattice site $\vec{r}'$ (these labels are suppressed in the following for sake of brevity), $\vec{r}$ is the distance from a chosen site, and $m_{\alpha\beta} = \frac{m_\alpha m_\beta}{m_\alpha + m_\beta}$. A simple variational estimate for the Wannier functions, which results in an estimate for the parameters in Eqs. (19) and (20), is discussed in Appendix C.

The tight-binding regime for the Yb is achieved for $V_0/E_{R_c} \gtrsim 2$–3, where V_0 is the amplitude of the periodic potential, $E_{Rc} = \frac{\hbar^2 k_0^2}{2m}$ is the recoil energy, k_0 is the wave vector of the laser producing the optical lattice, and m is chosen conventionally to be the mass of the ^{171}Yb isotope. We consider V_0 up to $\approx 15 E_{R_c}$, where the tunneling coefficients are very small and tunneling dynamics are effectively suppressed. Assuming this interval for the ratio V_0/E_{R_c} and Eqs. (19) and (20) with their optimized Wannier wave functions, the regions on the diagram U_c/U_{cf}, U_f/U_{cf} associated with the considered Yb mixture with natural interactions can be calculated.

In Fig. 6 we report on the left panel the hopping coefficients for different rescaled depths $\tilde{V}_0 = V_0/E_{Rc}$. We see that, also considering the small difference in mass between the two isotopes, one has $\Delta t/t \lesssim 10^{-1}$ so that the previous assumption $t_c = t_f \equiv t$ (however, not strictly required for the TFSL mechanism) is reasonable. On the right panel of the same figure we report the variation of $U_{\alpha,\beta}/t$, again as functions of $\tilde{V}_0 = V_0/E_{Rc}$. In the same way, the region in the diagram $U_{c,f}/U_{cf}$ associated with the Yb mixture can also be calculated. More details on the calculation are given in Appendix C.

If we write the intrapair interactions in the form $U_{c,f}/U_{cf}$, we observe that the dependence on the amplitude V_0 effectively drops out such that only the relative value of U_{cf}/t changes significantly and the obtained region resembles a single point.

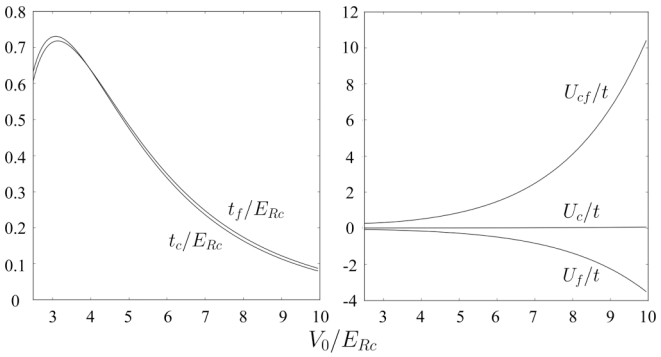

FIG. 6. Parameters of the Hamiltonian in Eq. (1), referred to the Yb mixture, as a function of the depth of the optical lattice potential $\tilde{V}_0 = V_0/E_{Rc}$. Left panel: hopping parameters t_c/E_{Rc} and t_f/E_{Rc}. Right panel: rescaled interaction parameters $U_{c,f}/t_c$ and U_{cf}/t_c.

This is the reason why we can speak about just a "natural point" in the diagrams of Figs. 2 and 5. This point is given approximately by the coordinates $U_c/U_{cf} \approx 0.01$ and $U_f/U_{cf} \approx -0.34$, also very close to the point estimated using the approximation $U_\alpha/U_{cf} \simeq a_\alpha/a_{cf}$ valid in the continuous space limit.

Importantly the natural point falls well inside the TFSL regime; see Figs. 2 and 5. In particular, along the line $U_c/t = 0$ [case (b) in Sec. IV], where the point almost lies, an estimate for the appearance of the antiferromagnetic regime can be done comparing the energies in Eqs. (10) and (18). As a result, the transition is located by the strong-coupling approach at the values $U_c/U_{cf} = -3.97$ for $U_{cf}/t = 3$, $U_c/U_{cf} \approx -4.9$ for $U_{cf}/t = 5$, and $U_c/U_{cf} \approx -5.6$ for $U_{cf}/t = 15$, in all the three cases far from the natural point of the Yb, that we recall to be $U_f/U_{cf} \approx -0.34$. In this way, our findings indicate that the TFSL phase can be observed in the zero-temperature limit in experiments with Yb mixtures, assuming natural interactions and realistic values for the depth of the lattice potential.

Despite the zero-temperature results reported, the TFSL phase could still be unreachable in the presence of a critical temperature (at fixed interactions), required for its occurrence, smaller than the ones currently realizable in the experiments. This point is particular important in the light of the mentioned difficulty to tune the interactions in earth-alkaline atoms. In the following, we estimate the critical temperature for the Yb mixture, proceeding as for the two-component attractive Hubbard model in Ref. [54], where the results are given as function of the total bandwidth. Here we refer to the case of isotropic hoppings t ($t_\perp = t_\parallel = t$ in the notation of [54]) and to the half-filling case. Moreover, $\tilde{\mu}_c = \tilde{\mu}_f$, as we found in Sec. III.

For our model on a cube lattice the total bandwidth is $D = 12t$. If we consider, for instance, $V_0 = 5E_{Rc}$, we obtain $2U_{cf} \approx 0.3D$, which results in $T_c K_B/D \approx 0.05$. Using these values and considering a lattice spacing of $a = 0.5$ μm, the critical temperature turns out to be $T_c \approx 15$ nK. In terms of the Fermi temperature this amounts to $T_c/T_F \approx 0.1$. This value is reasonably close to the ones achievable in current experiments [55], suggesting that the critical temperature assuming the natural interaction is reachable with current-day experiments and the TFSL phase could be achieved.

The lattice ratio $T_c/T_F \approx 0.1$ can be compared with the typical one for experiments in the continuous space, finding that apparently on the lattice T_c/T_F is larger. Indeed a very simple estimate can be done using the results [56] for a two-component mixture (as it is effectively the TFSL phase). Considering a number of loaded atoms $N \approx 10^4$ and a system size $\ell \sim 10\ \mu$m, one obtains T_c/T_F smaller than 0.01. This value is far from the presently achievable ones, different from the lattice case. Summing up, the present analysis suggests that, for the task to synthesize a TFSL phase in Yb mixtures, the use of a (cubic) lattice can be advantageous.

VI. CONCLUSIONS

In this paper we are motivated by the possibility to realize unconventional non-Abelian superfluid states using multicomponent fermionic mixtures. We investigated the emergence of a non-Abelian two-flavor locking (TFSL) superfluid phase in ultracold Fermi mixtures with four components and unequal interactions, showing that such states could be studied in current day experiments with ^{171}Yb-^{173}Yb mixtures. More in detail, using mean-field and strong-coupling results, we explored the phase diagram of this mixture loaded in a cubic lattice, finding for which ranges of the interactions and of the lattice width the system exhibits a TFSL phase.

These ranges are found to have an extended overlap with the ones realizable in current experiments. In particular, as detailed in the text, the proposed setup and phase are found to be realistic and realizable using a mixture of ^{171}Yb and ^{173}Yb. The phase diagram has been studied and the point in the phase diagram associated to the natural (not tuned) interactions between these atomic species determined. The latter ingredient is central for a possible experiment aiming to realize the TFSL phase, especially due to the known difficulty to tune interactions in earth-alkaline atomic gases, without spoiling their peculiar U(N) invariance. The critical temperature required for the appearance of the TFSL superfluid has been found comparable with the ones currently achievable.

We finally observe that for our results it is crucial that relatively large intrapair repulsions do not destroy the superfluid states. A different scenario is expected to take place when nonlocal repulsive interactions are present, the effects of which can be considered an interesting subject of future work.

ACKNOWLEDGMENTS

The authors are pleased to thank F. Becca, A. Celi, L. Fallani, M. Mannarelli, F. Minardi, L. Salasnich, and W. Vinci for useful discussions.

APPENDIX A: c AND f STRONGLY COUPLED LIMIT

In this Appendix we present details of the perturbative calculation for the strongly coupled limit in the presence of repulsive intrapair interactions, leading to Eq. (16) in the main text. We consider half filling.

The described physical situation corresponds to considering the Hamiltonian $H_0 + H_1$, where

$$H_0 = 2\sum_i (|U_c| n_{ir} n_{ig} + |U_f| n_{iu} n_{id}) - 2|U_{cf}| \sum_{i,c,f} n_{ic} n_{if}, \tag{A1}$$

$$H_1 = -t \sum_{\langle i,j\rangle,\sigma} c^\dagger_{i\sigma} c_{j\sigma}, \tag{A2}$$

and performing perturbation theory in the parameters $\varepsilon_c, \varepsilon_f \ll 1$ with $\varepsilon_c = t/|U_c|, \varepsilon_f = t/|U_f|$. We assume $\varepsilon_c = \varepsilon_f = \varepsilon$. The ground states of H_0, with energies $E = -2V|U_{cf}| = -N|U_{cf}|$, are the states where no single site is doubly occupied by intrapairing atoms, provided that $|U_{c,f}| > 3/2\,|U_{cf}|$. Let $\hat{G}$ be the projector on this space and $\hat{P} = 1 - \hat{G}$.

The lowest-order correction to E comes at the second order from the virtual process consisting in the interchange of location of two particles at nearest-neighbor distance. The calculation simplifies once we note that $\hat{P} H_1 = H_1$ and that $H_1|\phi\rangle$ is an eigenvector of H_0, with ϕ being one of its (degenerate) ground states. The related second-order effective Hamiltonian then is found to be

$$H_{\text{eff}} = \frac{t^2}{4} \sum_{\langle i,j\rangle} \left(\frac{1}{|U_c|} \vec{C}_i \cdot \vec{C}_j + \frac{1}{|U_f|} \vec{F}_i \cdot \vec{F}_j \right) - \frac{zNt^2}{8} \left(\frac{1}{|U_c|} + \frac{1}{|U_f|} \right), \tag{A3}$$

where $\vec{C}$ and $\vec{F}$ are the associated spin variables defined by $\vec{S}_i = \sum_{\sigma\sigma'} c^\dagger_{i\sigma} \vec{\tau}_{\sigma\sigma'} c_{i\sigma'}$, with the indices σ and σ' running through the labels c or f. The corresponding ground-state energy correction is $\Delta E = -\frac{zNt^2}{4}(\frac{1}{|U_c|} + \frac{1}{|U_f|})$, with z being the adjacency number for every site. In this way the ground-state energy at the second-order perturbation theory in $\frac{t}{U_{c,f}}$ becomes

$$E = -N|U_{cf}| - \frac{zNt^2}{4} \left(\frac{1}{|U_c|} + \frac{1}{|U_f|} \right). \tag{A4}$$

This formula is Eq. (17) of the main text.

APPENDIX B: STRONGLY COUPLED f AND WEAKLY COUPLED c

In this case the system is described by the Hamiltonian (in the same notation of Appendix A) $H_0 + H_1 + H_2$, where

$$H_0 = 2|U_f| \sum_i \hat{n}_{iu} \hat{n}_{id} - 2|U_{cf}| \sum_{i,c,f} \hat{n}_{ic} \hat{n}_{if} - t \sum_{\langle i,j\rangle,c} c^\dagger_{ic} c_{jc}, \tag{B1}$$

$$H_1 = -t \sum_{\langle i,j\rangle,f} c^\dagger_{if} c_{jf}, \quad H_2 = -2U_c \sum_i n_{ir} n_{ig}, \tag{B2}$$

with the perturbative parameters being $\varepsilon_1 = \frac{t}{|U_f|}$ and $\varepsilon_2 = \frac{|U_c|}{t}$. The ground state of H_0 can be derived in this limit assuming a basis of localized f degrees of freedom. Using such a basis, we can get an effective Hamiltonian for the c degrees

of freedom corresponding to noninteracting fermions in a one-body potential, in turn depending on the f configuration.

If $|U_f| \gg t$ and $|U_f| \gg |U_{cf}|$, the dynamics is dominated by the localization of the f atoms and therefore the ground state does not host any doubly occupied site. In that case in the ground state of H_0 a single f particle is in each site; therefore, the one-body potential felt by the c particles is site independent: $-2|U_{cf}|\hat{n}_{ic}$. The effect of this potential is to induce a shift $\delta\mu_c = -2\,|U_{cf}|$. Up to the first order of perturbation, the ground-state energy then results in $E_{0c} = 2\sum_{\vec{k}:\varepsilon_{\vec{k}}<0}\varepsilon_{\vec{k}}$. Instead the first order in ε_1 vanishes because it is related with forbidden double occupancies of sites by particles of the same species.

At the second order in ε_1 and ε_2, an effective Hamiltonian can be derived:

$$\begin{aligned}\hat{H}_{\rm eff} = \hat{G}\Bigg[&\varepsilon_1^2\hat{H}_1\frac{1}{(E_0-\hat{H}_0)}\hat{P}\hat{H}_1\\&+\varepsilon_1\varepsilon_2\left(\hat{H}_1\frac{1}{(E_0-\hat{H}_0)}\hat{P}\hat{H}_2+\text{H.c.}\right)\\&+\varepsilon_2^2\hat{H}_2\frac{1}{(E_0-\hat{H}_0)}\hat{P}\hat{H}_2\Bigg]\hat{G}\,,\end{aligned}\tag{B3}$$

with $\hat{G}$ and $\hat{P} = 1-\hat{G}$ as before. The term $\propto \varepsilon_1\varepsilon_2$ vanishes for the same reason for which the linear term in ε_1 does, and the remaining effective terms are then proportional to ε_2, ε_1^2, and ε_2^2. These terms commute with each other, so we can focus on them individually. After some algebra we arrive at the energy correction up to the second order for the ground-state energy:

$$\Delta E = N\left(-\frac{U_c}{4}-\frac{zt^2}{4}|U_f|-\frac{U_c^2}{t}\tilde{E}^{(2)}\right),\tag{B4}$$

where $\tilde{E}^{(2)}$ is a dimensionless positive quantity:

$$\tilde{E}^{(2)} = -\frac{1}{V^3}\sum_{\substack{\vec{k}_1,\vec{k}_2\,\in\,\mathbb{F}_S\\ \vec{q}_1,\vec{q}_2\,\notin\,\mathbb{F}_S}}\frac{\delta_{\vec{k}_1+\vec{k}_2\vec{q}_1+\vec{q}_2}}{\tilde{\varepsilon}_{\vec{k}_1}+\tilde{\varepsilon}_{\vec{k}_2}-\tilde{\varepsilon}_{\vec{q}_1}-\tilde{\varepsilon}_{\vec{q}_2}},\tag{B5}$$

with $\mathbb{F}_S$ labeling the set of points of the Fermi sea and $\tilde{\varepsilon_k} = \varepsilon_k/2t$. Equation (B5) is used to arrive at Eq. (18) of the main text, where $U_c = 0$ and the calculation of $\tilde{E}^{(2)}$ is not required.

APPENDIX C: DETERMINATION OF THE MODEL PARAMETERS

In this Appendix we perform a variational estimate of the parameters entering in the Hamiltonian (1), which can be obtained from the expressions

$$\begin{aligned}t_{ij\alpha} =& -\int d^3\vec{r}\left(\frac{\hbar^2}{2m_\alpha}\nabla\phi_{i\alpha}(\vec{r})\cdot\nabla\phi_{j\alpha}(\vec{r})\right.\\&\left.+\phi_{i\alpha}(\vec{r})V_{\rm ext}(\vec{r})\phi_{j\alpha}(\vec{r})\right),\\U_{\alpha\beta} =& -\frac{\pi\hbar^2 a_{\alpha\beta}}{m_{\alpha\beta}}\int d^3\vec{r}|\phi_\alpha(\vec{r})|^2|\phi_\beta(\vec{r})|^2.\end{aligned}\tag{C1}$$

$V_{\rm ext}(\vec{r}) = V_0\sum_{j=1}^3\sin^2(k_0 r_i)$ is the external potential creating the lattice ($k_0 = \frac{2\pi}{a}$, a being the lattice spacing), $a_{\alpha\beta}$ corresponds to the scattering lengths between the α and β species, and $m_{\alpha\beta}$ are their reduced masses. Moreover, the $\phi_\alpha(\vec{r})$ refer to the Wannier functions centered on the lattice sites. A simple estimate of these functions can be obtained by variational approach. In particular, we consider the following ansatz:

$$\phi_\alpha(\vec{r}) = C_\alpha e^{-\frac{|\vec{r}|^2}{2\sigma_\alpha^2}},\tag{C2}$$

where $C_\alpha = (\sqrt{\pi}\sigma_\alpha)^{-3/2}$. The values of the coefficients σ_α are fixed by minimizing the energy per lattice site. This energy can be found as the expectation value of the Hamiltonian (1) acting on the multiparticle fermionic state $\Psi_\alpha(\vec{r}_1,\ldots,\vec{r}_V)$ (V being the number of lattice sites, at half filling equal to the number of c or f atoms) constructed by the Wannier functions. In the mean-field approximation it reads

$$\begin{aligned}\varepsilon = \int\prod_{i=1}^V d^3\vec{r}_i\Bigg(&\sum_\alpha\frac{\hbar^2}{2m_\alpha}|\nabla\Psi_\alpha|^2+V_{\rm ext}|\Psi_\alpha|^2\\&+\sum_{\beta>\alpha}\frac{2\pi\hbar^2 a_{\alpha\beta}}{m_{\alpha\beta}}|\Psi_\alpha|^2|\Psi_\beta|^2\Bigg).\end{aligned}\tag{C3}$$

Using the (approximate) orthogonality of the Wannier functions at different lattice sites one obtains

$$\begin{aligned}\varepsilon = \int d^3\vec{r}\sum_{\vec{r}',\alpha}\Bigg(&n_\alpha\frac{\hbar^2}{2m_\alpha}|\nabla\phi_{\alpha\vec{r}'}|^2+n_\alpha V_{\rm ext}|\phi_{\alpha\vec{r}'}|^2\\&+\sum_{\beta>\alpha}n_\alpha n_\beta\frac{g_{\alpha\beta}}{2}|\phi_{\alpha\vec{r}'}|^2|\phi_{\beta\vec{r}'}|^2\Bigg),\end{aligned}\tag{C4}$$

with $n_{\{\alpha,\beta\}}$ being the average number of particles of $\{\alpha,\beta\}$ per site and $g_{\alpha\beta} = \frac{4\pi\hbar^2 a_{\alpha\beta}}{m_{\alpha\beta}}$. Moreover, the Wannier functions, centered on the lattice sites labeled by $\vec{r}\,'$, depend on the space vector $\vec{r}$ spanning all the lattice. Using the ansatz in Eq. (C2) one finds

$$\begin{aligned}\varepsilon/N = \sum_\alpha\Bigg[&n_\alpha\frac{\hbar^2}{2m_\alpha}\frac{3}{2\sigma_\alpha^2}+n_\alpha\frac{3V_0}{2}\left(1-e^{-k_0^2\sigma_\alpha^2}\right)\\&+\sum_{\beta>\alpha}n_\alpha n_\beta\frac{g_{\alpha\beta}}{2\pi^{3/2}\left(\sigma_\alpha^2+\sigma_\beta^2\right)^{3/2}}\Bigg].\end{aligned}\tag{C5}$$

Imposing $\frac{\partial\varepsilon}{\partial\sigma_\mu} = 0$ and expressing the parameters in Eq. (C5) as adimensional quantities $\tilde{\sigma}_\mu = k_0\sigma_\mu$, $\tilde{V}_\alpha = \frac{V_0}{E_R^\alpha}$, and $\tilde{a}_{\alpha\beta} = k_0 a_{\alpha\beta}$, with $E_R^\alpha = \frac{\hbar^2 k_0^2}{2m_\alpha}$, the result is a set of coupled equations:

$$\frac{1}{\tilde{\sigma}_\mu^3}-\tilde{V}_\mu\tilde{\sigma}_\mu e^{-\tilde{\sigma}_\mu^2}+4\sum_{\beta\neq\mu}n_\beta\left(1+\frac{m_\mu}{m_\beta}\right)\frac{\tilde{a}_{\mu\beta}\tilde{\sigma}_\mu}{\sqrt{\pi}\left(\tilde{\sigma}_\mu^2+\tilde{\sigma}_\beta^2\right)^{5/2}}=0.\tag{C6}$$

Solving this set in $\{\sigma_\alpha\}$, the Hubbard coefficients are finally obtained by substituting the solutions in

$$\begin{aligned}t_\alpha =& -\left\{\frac{\hbar^2}{2m_\alpha}\frac{1}{4\sigma_\alpha^2}\left[6-\left(\frac{a}{\sigma_\alpha}\right)^2\right]+\frac{V_0}{2}\left(3-e^{-k_0^2\sigma_\alpha^2}\right)\right\}e^{-\frac{a^2}{4\sigma_\alpha^2}},\\U_{\alpha\beta} =& -\frac{\hbar^2 a_{\alpha\beta}}{\sqrt{\pi}m_{\alpha\beta}}\frac{1}{\left(\sigma_\alpha^2+\sigma_\beta^2\right)^{3/2}}.\end{aligned}\tag{C7}$$

For the case of the Yb mixture the interactions are the same for the species r,g and u,d, resulting in two equations (for $\tilde{\sigma_c}$ and $\tilde{\sigma_f}$):

$$\frac{1}{\tilde{\sigma}_c^3} - \tilde{V}_c\tilde{\sigma}_c e^{-\tilde{\sigma}_c^2} + \frac{n_c\tilde{a}_{cc}}{\sqrt{2\pi}\tilde{\sigma}_c^4} + \left(1+\frac{m_c}{m_f}\right)\frac{4n_f\tilde{a}_{cf}\tilde{\sigma}_c}{\sqrt{\pi}\left(\tilde{\sigma}_c^2+\tilde{\sigma}_f^2\right)^{5/2}} = 0,$$
$$\frac{1}{\tilde{\sigma}_f^3} - \tilde{V}_f\tilde{\sigma}_f e^{-\tilde{\sigma}_f^2} + \frac{n_f\tilde{a}_{ff}}{\sqrt{2\pi}\tilde{\sigma}_f^4} + \left(1+\frac{m_f}{m_c}\right)\frac{4n_c\tilde{a}_{cf}\tilde{\sigma}_f}{\sqrt{\pi}\left(\tilde{\sigma}_c^2+\tilde{\sigma}_f^2\right)^{5/2}} = 0. \quad \text{(C8)}$$

The solutions are presented in Fig. 6 of the main text for the symmetric case $n_c = n_f \equiv n = 1$.

[1] I. Bloch, J. Dalibard, and W. Zwerger, Rev. Mod. Phys. **80**, 885 (2008).
[2] M. Lewenstein, A. Sanpera, and V. Ahufinger, *Ultracold Atoms in Optical Lattices: Simulating Quantum Many-body Systems* (Oxford University Press, Oxford, 2012).
[3] J. Dalibard, F. Gerbier, G. Juzeliūnas, and P. Öhberg, Rev. Mod. Phys. **83**, 1523 (2011).
[4] M. Greiner, O. Mandel, T. Esslinger, T. W. Hänsch, and I. Bloch, Nature (London) **415**, 39 (2002).
[5] F. S. Cataliotti, S. Burger, C. Fort, P. Maddaloni, F. Minardi, A. Trombettoni, A. Smerzi, and M. Inguscio, Science **293**, 843 (2001).
[6] T. Esslinger, Annu. Rev. Condens. Matter Phys. **1**, 129 (2010).
[7] F. Gerbier and J. Dalibard, New J. Phys. **12**, 033007 (2010).
[8] E. Zohar, J. I. Cirac, and B. Reznik, Phys. Rev. Lett. **109**, 125302 (2012); **110**, 055302 (2013); **110**, 125304 (2013).
[9] D. Banerjee, M. Dalmonte, M. Müller, E. Rico, P. Stebler, U.-J. Wiese, and P. Zoller, Phys. Rev. Lett. **109**, 175302 (2012).
[10] L. Tagliacozzo, A. Celi, A. Zamora, and M. Lewenstein, Ann. Phys. (NY) **330**, 160 (2013).
[11] D. Banerjee, M. Bögli, M. Dalmonte, E. Rico, P. Stebler, U.-J. Wiese, and P. Zoller, Phys. Rev. Lett. **110**, 125303 (2013).
[12] M. J. Edmonds, M. Valiente, G. Juzeliūnas, L. Santos, and P. Öhberg, Phys. Rev. Lett. **110**, 085301 (2013).
[13] E. A. Martinez, C. A. Muschik, P. Schindler, D. Nigg, A. Erhard, M. Heyl, P. Hauke, M. Dalmonte, T. Monz, P. Zoller, and R. Blatt, Nature (London) **534**, 516 (2016).
[14] N. Nagaosa, *Quantum Field Theory in Condensed Matter Physics* (Springer-Verlag, Berlin, 1999).
[15] D. Jaksch and P. Zoller, New J. Phys. **5**, 56 (2003).
[16] K. Osterloh, M. Baig, L. Santos, P. Zoller, and M. Lewenstein, Phys. Rev. Lett. **95**, 010403 (2005).
[17] M. Aidelsburger, M. Atala, S. Nascimbène, S. Trotzky, Y.-A. Chen, and I. Bloch, Phys. Rev. Lett. **107**, 255301 (2011).
[18] K. Jimenez-Garcia, L. J. Le Blanc, R. A. Williams, M. C. Beeler, A. R. Perry, and I. B. Spielman, Phys. Rev. Lett. **108**, 225303 (2012).
[19] P. Hauke, O. Tieleman, A. Celi, C. Ölschläger, J. Simonet, J. Struck, M. Weinberg, P. Windpassinger, K. Sengstock, M. Lewenstein, and A. Eckardt, Phys. Rev. Lett. **109**, 145301 (2012).
[20] S.-L. Zhu, B. Wang, and L.-M. Duan, Phys. Rev. Lett. **98**, 260402 (2007).
[21] B. Wunsch, F. Guinea, and F. Sols, New J. Phys. **10**, 103027 (2008).
[22] C. Wu and S. D. Sarma, Phys. Rev. B **77**, 235107 (2008).
[23] G. Juzeliūnas, J. Ruseckas, M. Lindberg, L. Santos, and P. Öhberg, Phys. Rev. A **77**, 011802(R) (2008).
[24] L.-K. Lim, C. M. Smith, and A. Hemmerich, Phys. Rev. Lett. **100**, 130402 (2008).
[25] J.-M. Hou, W.-X. Yang, and X.-J. Liu, Phys. Rev. A **79**, 043621 (2009).
[26] K. L. Lee, B. Grémaud, R. Han, B.-G. Englert, and C. Miniatura, Phys. Rev. A **80**, 043411 (2009).
[27] E. Alba, X. Fernandez-Gonzalvo, J. Mur-Petit, J. J. Garcia-Ripoll, and J. K. Pachos, Ann. Phys. (NY) **328**, 64 (2013).
[28] L. Lamata, J. Léon, T. Schätz, and E. Solano, Phys. Rev. Lett. **98**, 253005 (2007).
[29] L. Lepori, G. Mussardo, and A. Trombettoni, Europhys. Lett. **92**, 50003 (2010).
[30] L. Mazza, A. Bermudez, N. Goldman, M. Rizzi, M. A. Martin-Delgado, and M. Lewenstein, New J. Phys. **14**, 015007 (2012).
[31] L. Lepori, A. Trombettoni, and W. Vinci, Europhys. Lett. **109**, 50002 (2015).
[32] V. Kasper, F. Hebenstreit, M. Oberthaler, and J. Berges, Phys. Lett. B **760**, 742 (2016).
[33] L. Tarruell, D. Greif, T. Uehlinger, G. Jotzu, and T. Esslinger, Nature (London) **483**, 302 (2012).
[34] G. Jotzu, M. Messer, R. Desbusquois, M. Lebrat, T. Uehlinger, D. Greif, and T. Esslinger, Nature (London) **515**, 237 (2014).
[35] *The BCS-BEC Crossover and the Unitary Fermi Gas*, edited by W. Zwerger (Springer, Heidelberg, 2012).
[36] *Novel Superfluids*, edited by K. H. Bennemann and J. B. Ketterson (Oxford University Press, Oxford, 2014).
[37] M. Alford, A. Schmitt, K. Rajagopal, and T. Schäfer, Rev. Mod. Phys. **80**, 1455 (2008).
[38] R. Anglani, R. Casalbuoni, M. Ciminale, R. Gatto, N. Ippolito, M. Mannarelli, and M. Ruggieri, Rev. Mod. Phys. **86**, 509 (2014).
[39] R. Auzzi, S. Bolognesi, J. Evslin, K. Konishi, and A. Yung, Nucl. Phys. B **673**, 187 (2003).
[40] R. Auzzi, S. Bolognesi, J. Evslin, K. Konishi, and H. Murayama, Nucl. Phys. B **701**, 207 (2004).
[41] M. Shifman and A. Yung, Phys. Rev. D **70**, 045004 (2004).
[42] A. Hanany and D. Tong, J. High Energy Phys. 07 (2003) 037.
[43] M. Eto, Y. Isozumi, M. Nitta, K. Ohashi, and N. Sakai, Phys. Rev. Lett. **96**, 161601 (2006).
[44] M. Alford, K. Rajagopal, and F. Wilczek, Nucl. Phys. B **537**, 443 (1999).
[45] G. Pagano, M. Mancini, G. Cappellini, P. Lombardi, F. Schäfer, H. Hu, X.-J. Liu, J. Catani, C. Sias, M. Inguscio, and L. Fallani, Nat. Phys. **10**, 198 (2014).

[46] A. V. Gorshkov, M. Hermele, V. Gurarie, C. Xu, P. S. Julienne, J. Ye, P. Zoller, E. Demler, M. D. Lukin, and A. M. Rey, Nat. Phys. **6**, 289 (2010).

[47] S. Taie, Y. Takasu, S. Sugawa, R. Yamazaki, T. Tsujimoto, R. Murakami, and Y. Takahashi, Phys. Rev. Lett. **105**, 190401 (2010).

[48] S.-K. Yip, Phys. Rev. A **83**, 063607 (2011).

[49] S. Weinberg, *The Quantum Theory of Fields* (Cambridge University Press, Cambridge, UK, 1996), Vol. 2.

[50] C. J. Pethick and H. Smith, *Bose-Einstein Condensation in Diluite Gases*, 2nd ed. (Cambridge University Press, Cambridge, UK, 2008), Chap. 16.

[51] E. Fradkin, *Field Theories of Condensed Matter Physics* (Cambridge University Press, Cambridge, UK, 2013).

[52] M. Mannarelli, G. Nardulli, and M. Ruggieri, Phys. Rev. A **74**, 033606 (2006).

[53] G. Pagano, M. Mancini, G. Cappellini, L. Livi, C. Sias, J. Catani, M. Inguscio, and L. Fallani, Phys. Rev. Lett. **115**, 265301 (2015).

[54] M. Iazzi, S. Fantoni, and A. Trombettoni, Europhys. Lett. **100**, 36007 (2012).

[55] G. Valtolina, A. Burchianti, A. Amico, E. Neri, K. Xhani, J. A. Seman, A. Trombettoni, A. Smerzi, M. Zaccanti, M. Inguscio, and G. Roati, Science **350**, 1505 (2015).

[56] W. Ketterle and M. W. Zwierlein, Making, probing and understanding ultracold Fermi gases, in *Proceedings of the International School of Physics "Enrico Fermi", Course CLXIV, Varenna, 2006*, edited by M. Inguscio, W. Ketterle, and C. Salomon (IOS Press, Amsterdam, 2008).